Local Negative Shear and the Formation of Transport Barriers

J. F. Drake, Y. T. Lau, P. N. Guzdar, A. B. Hassam, S. V. Novakovski, B. Rogers, and A. Zeiler*
Institute for Plasma Research, University of Maryland, College Park, Maryland 20742
(Received 12 March 1996)

We present a set of 3D nonlinear equations describing drift-resistive ballooning modes in a torus including the self-consistent modification of the local magnetic shear due to the finite β shift of the flux surfaces. Simulations using these equations reveal that a bifurcation of the transport occurs when the local magnetic shear on the outside midplane reverses sign. A fully self-consistent bifurcation diagram is calculated which reveals significant hysteresis, i.e., the transport barrier is maintained at lower values of β than is required for the formation of the barrier, as expected from the experimental observations. [S0031-9007(96)00616-3]

PACS numbers: 52.30.Jb, 52.35.Kt, 52.55.Fa

Energy confinement in tokamaks and other plasma fusion experiments is always lower than can be explained by transport by classical interparticle collisions. The observation of the formation of transport barriers in tokamaks first in the plasma periphery during the *L-H* transition [1,2] and more recently in the core [3–6] has provided strong evidence that transport can be controlled. The development of an understanding of the underlying causes of these barriers is critical if we are to be able to have confidence in our ability to maximize their benefit in improving confinement. The leading model to explain the *L-H* transition is based on sheared flow generation and the associated stabilization of turbulence [7,8]. However, experimental evidence supporting the role of sheared flow on the transition is contradictory [9,10]. More recently, suggestions that negative magnetic shear would stabilize fluctuations and improve confinement [11] were dramatically confirmed on experiments in D-IIID [6] and TFTR [5] and led to renewed interest in the role of magnetic shear on toroidal instabilities. The mechanism for reversed shear stabilization has been identified as the poloidal twisting of radially extended curvature driven fluctuations [12].

In this Letter we suggest that local negative magnetic shear may in fact underlie the formation of transport barriers which form both in the plasma edge during the *L-H* transition and in the plasma core. It is well known that the compression of poloidal magnetic flux on the large major radius side of a toroidal plasma causes the magnetic shear to locally reverse if the pressure gradient is sufficiently large. We demonstrate that this toroidally induced negative shear stabilizes drift-resistive ballooning modes, which have been identified as the likely mechanism for anomalous transport in the plasma edge [13,14]. Further we present a set of model equations which self-consistently describe the full 3D evolution of drift-resistive ballooning modes coupled with the evolution of the ambient pressure gradient and the shift of the magnetic flux surfaces. These equations are strictly valid only in the collisional edge plasma. Simulations completed with these equations reveal a transport bifurcation which arises as the pressure increases and the local magnetic shear on the outside of the torus reverses. A similar idea based on the change in the direction of precession of trapped particles is being explored by others [15].

The calculations are carried out in a flux tube based coordinate system consisting of a poloidally and radially localized domain which winds around the torus [14]. In a simple shifted circle model, the coupled equations for perturbations of the density n, potential ϕ, and parallel flow v_z are given by

$$\frac{dn}{dt} + \frac{\partial \phi}{\partial y} - \epsilon_n C(\phi - \alpha_d n) + \alpha_d \epsilon_n \frac{\partial^2}{\partial z^2}(\phi - \alpha_d n) + \gamma \frac{\partial v_z}{\partial z} = 0, \tag{1}$$

$$\frac{d}{dt}\nabla_\perp^2 \phi + Cn + \frac{\partial^2}{\partial z^2}(\phi - \alpha_d n) = 0, \tag{2}$$

$$\frac{dv_z}{dt} + \gamma \frac{\partial n}{\partial z} = 0, \tag{3}$$

where $T_i = 0$ and T_e is assumed to be a constant, C is the curvature operator,

$$C = [\cos(2\pi z) + h(z)\sin(2\pi z) - \epsilon]\frac{\partial}{\partial y} + \sin(2\pi z)\frac{\partial}{\partial x}, \tag{4}$$

$$\nabla_\perp^2 = \left(\frac{\partial}{\partial x} + h(z)\frac{\partial}{\partial y}\right)^2 + \frac{\partial^2}{\partial y^2}, \tag{5}$$

$$h(z) = 2\pi \hat{s} z - \alpha \sin(2\pi z), \tag{6}$$

$$\frac{d}{dt} = \frac{\partial}{\partial t} + \hat{z} \times \nabla\phi \cdot \nabla,$$

where z lies along $\mathbf{B}$, the ambient density gradient is in the x direction and the y direction is defined by $\mathbf{B} \cdot \nabla y = 0$. The equations have been normalized using $L_z = 2\pi qR$ as the parallel scale length, $L_0 = 2\pi q(\nu_{ei} R\rho_s/2\Omega_e)^{1/2} \times (2R/L_n)^{1/4}$ as the transverse scale and the ideal ballooning growth time, $t_0 = (RL_n/2)^{1/2}/c_s$, as the time. In these

 0031-9007/96/77(3)/494(4)$10.00

normalized units $n/n_0 \sim v_z/c_s \sim L_0/L_n$, $\phi \sim BL_0^2/ct_0$ and the transport scales like

$$D_0 = (2\pi q)^2 \rho_e^2 \nu_{ei} R/L_n \,. \tag{7}$$

Other parameters are $\epsilon_n = 2L_n/R$, the inverse aspect ratio $\epsilon = a/R$, the diamagnetic parameter $\alpha_d = \rho_s c_s t_0/L_n L_0$, and $\gamma = c_s t_0/L_z$ with L_n the equilibrium density (or pressure) scale length. Realistic diffusive dissipation terms are added to each equation to model ion viscosity and classical transport. The spatial-differencing and time-stepping schemes used to advance the equations have been described previously [14].

The key new ingredient in these equations is the toroidal shift induced magnetic shear which appears in the function $h(z)$ in (6). The standard flux surface averaged magnetic shear $\hat{s} = (dq/dx)a/q$ is now combined with the magnetic shear induced by the toroidal shift of the flux surfaces, proportional to $\alpha = a\epsilon d\beta_p/dx$. The toroidally induced shear is negative on the outside of the torus ($z \sim 0$) and positive on the inside ($z \sim 0.5$). Thus, for $\alpha > \hat{s}$ the local magnetic shear on the outside of the torus becomes negative. Negative magnetic shear generally has a stabilizing impact on both ideal and kinetic modes driven by curvature. The local negative shear produced by the toroidal shift of the flux surfaces is one of the factors causing second stability of ideal modes [16,17].

Since the impact of the pressure induced shear on the transport driven by resistive-ballooning modes has not been explored, we first present the results of such a study. Equations (1)–(3) are seeded with small perturbations and then advanced in time until the average properties of the turbulence reach a steady state. The particle flux $\Gamma = \langle n v_x \rangle$ can then be evaluated, where $\langle\ \rangle$ denotes a spatial average over the entire volume of the simulation domain. In Fig. 1 we plot Γ as a function of α from a series of simulations with parameters $L_z = 3.0$, $L_y = 8.0$, $L_x = 7.64$, $\hat{s} = 1.0$, $\alpha_d = 0.25$, $\epsilon_n = 0.1$, and $\gamma = 0.02$. The flux first increases with increasing α and then drops off sharply. The mechanism for stabilization is the

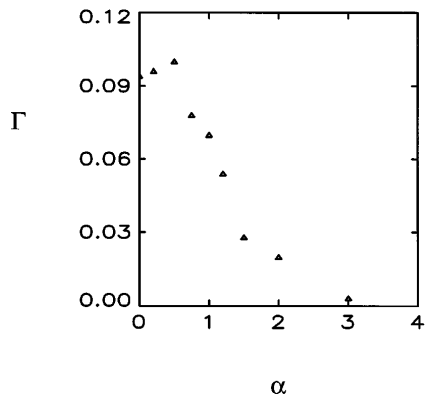

FIG. 1. The particle flux Γ versus α from a series of 3D simulations.

poloidal twisting of radial flows as discussed previously [12]. Thus, the pressure induced toroidal shift of the flux surfaces strongly reduces the transport driven by resistive-ballooning modes.

We now want to couple the transport with the toroidal shift of the surfaces calculated consistently with the local transport to explore how and when a bifurcation occurs. Specifically the bifurcation occurs as follows: a local increase of the plasma pressure gradient causes an increase of the toroidal shift and associated local negative shear; the increased negative shear stabilizes the turbulence and reduces transport; reduced transport causes the pressure gradient to increase. The critical value of β_p required for the bifurcation must be calculated from a more specific model, which we now present. Because of the periodic boundary conditions imposed in the radial direction, our edge turbulence code allows local evolution of the density profile but does not describe the evolution of a global profile. To study self-steepening, we therefore need to solve a separate model equation for the average gradient n'. For simplicity we treat the barrier as a region of fixed width, L_n, the density gradient scale length in the L mode, but with a time varying gradient n'. The total particle number in the layer is $N = n' L_n^2/2$. The rate of change of n' is calculated from $\partial N/\partial t$, which is given by the difference between the flux into the edge from the central core, $\Gamma_c + D_0 n_c'$, and the flux through the edge, $\Gamma + D_0 n'$, where D_0 is the neoclassical diffusion rate, n_c' is the gradient in the core just inside the edge, Γ_c being the anomalous flux in the same location, and Γ is the anomalous flux in the edge calculated from the 3D simulation. The resulting evolution equation for n' in dimensionless form is then

$$\frac{d}{dt} n' = (\Gamma_c + D_0 n_c' - \Gamma - D_0 n')/\tau_n \,, \tag{8}$$

where τ_n is the confinement time of the edge. In dimensionless units $\tau_n = L_n^2/L_0^2 \gg 1$ where the inequality follows because the characteristic time required for the gradient in the edge to change is much longer than the characteristic time scale of the turbulence. To feed the evolution of the gradient into the code, n' is inserted in front of the $\partial\phi/\partial y$ in the continuity equation (1) and $\alpha = \hat{\alpha} n'$ in the equation for the shear in (6). The control parameter in the nonlinear system is now $\hat{\alpha}$. Increasing $\hat{\alpha}$ corresponds to increasing β_p in the physical system. We take the flux Γ_c from the core into the edge to be fixed at the level given by $\alpha = 0.0$ in Fig. 1 with $n_c' = 1$ also fixed. The normalization is to the pretransition gradient. With $n' = 1.0$ initially, we then ramp up $\hat{\alpha}$ either very slowly in time or in small increments. Equation (8) evolves n' in time. If the flux through the edge drops below that from the core, the right side of (8) is positive and the gradient increases. In a stable situation the increased gradient increases the edge particle flux until

the equilibrium condition

$$\Gamma + D_0 n' = \Gamma_c + D_0 \tag{9}$$

is satisfied and n' remains stationary at a higher value. The stability of this equilibrium can be simply calculated by varying Eq. (8) with respect to a perturbation of the density gradient. The system is unstable if

$$\frac{d\Gamma}{dn'} = \frac{\partial \Gamma}{\partial n'} + \frac{\partial \Gamma}{\partial \alpha}\frac{\partial \alpha}{\partial n'} < -D_0 . \tag{10}$$

Normally, $\partial\Gamma/\partial n' > 0$ so this term is stabilizing. Specifically, in the resistive-ballooning regime where diamagnetic effects are small, $\Gamma \sim n'^2$. Figure 1 indicates that for α above 0.5 the toroidally induced shear reduces transport and therefore drives the bifurcation. In Fig. 2 we plot the diffusion rate $D = D_0 + \Gamma/n'$ and n' from a series of simulations with varying values of $\hat{\alpha}$, $D_0 = 0.2$, and other parameters as in Fig. 1. The diffusion remains high up to $\hat{\alpha} = 0.85$ and then begins to slowly decrease in parallel with a gradual rise in n'. Above $\hat{\alpha} = 0.972$ no steady state solution is found with high diffusion. In this regime the diffusion drops and n' increases until a new equilibrium is reached with low diffusion and a large gradient, i.e., $n' > 3$. The low diffusion solutions remain stable for values of $\hat{\alpha}$ down to 0.87. In this low diffusion regime the neoclassical and fluctuation driven diffusion contribute at comparable levels. The plus in Fig. 2 corresponds to an unstable equilibrium point, which was obtained by sweeping n' until the equilibrium condition in (9) was satisfied. Figure 2 clearly demonstrates that the transport undergoes a bifurcation due to the finite β shift of the flux surfaces in a torus. Following the usual convention, we refer to the high and low confinement solutions as the H and L modes. The bifurcation occurs for $\alpha = \hat{\alpha} n' = 1.2$ which for $\hat{s} = 1$ corresponds to a slightly negative local shear on the outside midplane. Surprisingly, the fluctuation level in the L and H modes at a fixed value of $\hat{\alpha}$ is virtually the same. Of course, in the H mode the density gradient is much larger than in the L mode and the rate of diffusion is much smaller. With increasing $\hat{\alpha}$ in the H mode the amplitude of the fluctuations rapidly decreases. The turbulence undergoes a change in character across the transition. The difference in the character of the turbulence can be seen in the grey-scale plots of the density fluctuations in the x-y plane shown in Fig. 3. The plots are both from simulations with $\hat{\alpha} = 0.96$ with (a) and (b) corresponding to the L and H modes, respectively. The fluctuations in (a) exhibit radially extended disturbances with distinct mushroomlike structures typical of resistive-ballooning driven turbulence [14]. In (b) the disturbances are smoother and have a shorter radial correlation length. In this regime, the fluctuations n and ϕ are also more strongly correlated, reducing the transport. If the curvature in the simulation in (b) is turned off, the fluctuations actually increase in amplitude. Linear stability calculations reveal that the strong modulation of the shear in the system allows drift waves to grow even in the absense of curvature. The instability therefore is distinct from the toroidal drift waves explored previously [18]. The transport associated with these instabilites is weak.

There is already substantial experimental evidence that local shear reversal plays a role in the formation of both

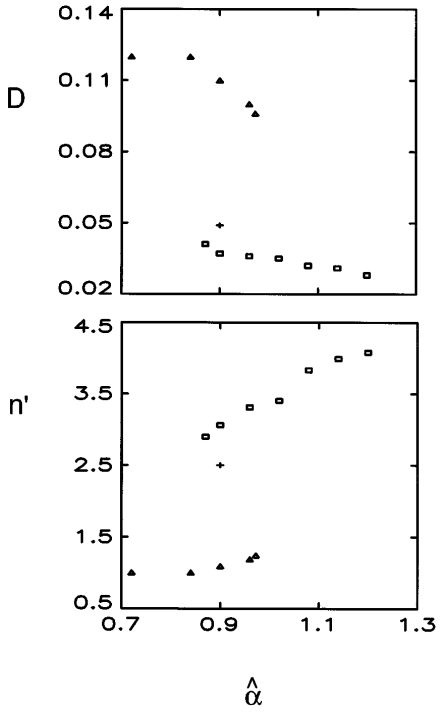

FIG. 2. The diffusion rate D and density gradient n' versus $\hat{\alpha}$ across the bifurcation.

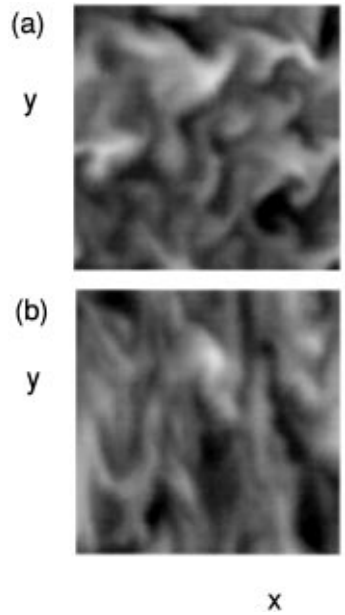

FIG. 3. Density fluctuations in (a) the L mode and (b) the H mode for $\hat{\alpha} = 0.96$.

edge and central transport barriers. Direct measurements of the radial profile of the vertical magnetic field B_z on the outside midplane of the DIII-D tokamak using the motional Stark effect (MSE) reveal that in the L mode the local magnetic shear in the edge is positive while it is negative in the H mode [19]. Analysis of pellet induced transport barriers in JET reveals that local reversed shear is produced by the steep pressure gradients in the core region [3]. The core high β_p transport barriers on JT60-U are observed to form near the magnetic axis and propagate outwards [4]. The genesis of the barrier in this region of weak average magnetic shear is qualitatively consistent with the threshold $\alpha \sim \hat{s}$ for the local shear to reverse, i.e., a small pressure gradient is required to reverse the local shear and form the barrier in a region where the average magnetic shear is small. Once the barrier forms the pressure induced reversed shear is large and the barrier can move radially outwards where the average positive shear is larger. Of course, this cannot be the whole story because there is still a power threshold which must be exceeded for the formation of internal barriers in tokamak discharges with negative average shear [5,6]. We emphasize again that resistive-ballooning modes are not unstable in the hot central core of tokamaks so that application of the present theory to this region can be only qualitative.

Two final issues concern the role of sheared flow and the stability of ideal pressure driven ballooning modes. Resistive-ballooning modes are unstable and drive transport in the edge of tokamaks at small values of α. The present theory suggests that these modes are stabilized by the local reversed magnetic shear when α exceeds a threshold. This theory requires that the stability threshold for ideal ballooning modes be above the α threshold for stabilization of the resistive modes. In a simple circular cross-section machine this gap may not even exist while in machines with modest elongation and triangularity the gap is substantial since the ideal β limit increases significantly or is absent [20]. The most complete models of the L-H transition are based on the stabilization of turbulence by sheared flow [7,8]. The present simulations include sheared flow but do not properly model the shear layer in the edge region. Thus our point is not to claim that sheared rotation cannot cause a bifurcation but to show that the local reversed shear is important in the formation of transport barriers.

This work was supported in part by the U.S. Department of Energy.

*Permanent address: Max-Planck-Institut für Plasmaphysik, EURATOM Association, 85748 Garching, Germany.

[1] F. Wagner *et al.*, Phys. Rev. Lett. **49**, 1408 (1982).
[2] K. Burrell *et al.*, Phys. Fluids B **2**, 1405 (1990).
[3] M. Hugon *et al.*, Nucl. Fusion **32**, 33 (1992).
[4] Y. Koide *et al.*, in *Plasma Physics and Controlled Nuclear Fusion Research* (IAEA, Vienna, 1994), Vol. 1, p. 199.
[5] F. M. Levinton *et al.*, Phys. Rev. Lett. **75**, 4417 (1995).
[6] E. J. Strait *et al.*, Phys. Rev. Lett. **75**, 4421 (1995).
[7] A. B. Hassam *et al.*, Phys. Rev. Lett. **66**, 309 (1991).
[8] P. H. Diamond *et al.*, in Ref. [4], paper D-2-II-6.
[9] K. Burrell *et al.*, in Ref. [4], Vol. I, p. 221.
[10] Winfried Herrmann and the Asdex Upgrade Team, Phys. Rev. Lett. **75**, 4401 (1995).
[11] C. Kessel *et al.*, Phys. Rev. Lett. **72**, 4420 (1994).
[12] T. M. Antonsen *et al.*, Phys. Plasmas Lett. **3**, 2221 (1996).
[13] P. N. Guzdar *et al.*, Phys. Fluids B **3**, 3712 (1993).
[14] A. Zeiler *et al.*, Phys. Plasmas (to be published).
[15] M. A. Beer and G. W. Hammett, Bull. Am. Phys. Soc. **40**, 1733 (1995).
[16] D. Lortz and J. Nuhrenberg, Phys. Lett. **68A**, 49 (1978).
[17] B. Coppi, A. Ferreira, and J. J. Ramos, Phys. Rev. Lett. **44**, 990 (1980).
[18] C. Z. Cheng and L. Chen, Phys. Fluids **23**, 2242 (1980).
[19] B. Rice *et al.*, Bull. Am. Phys. Soc. **39**, 1562 (1994).
[20] E. J. Strait, Phys. Plasmas **1**, 1415 (1994).